The Evolution of Plasmonic States from Visible Light to Microwaves

Minfeng Chen and Hung-chun Chang
Graduate Institute of Photonics and Optoelectronics,
Graduate Institute of Communication Engineering, and Department of Electrical Engineering
National Taiwan University, Taipei, Taiwan 10617, R.O.C.
hcchang@cc.ee.ntu.edu.tw

1. Introduction

The guiding of light below the diffraction limit has been an active research in recent years [1,2]. In designing these deep subwavelength photonic devices, the surface plasmon polaritons (SPPs) play a crucial role. The SPP is the coupling between photons and electrons. At a metal/dielectric boundary, the electromagnetic (EM) waves are strongly confined where the surface electrons simultaneously oscillate with electric fields. Extensive studies on light guidance utilizing the SPP have been reported. The simplest structure is known to be the metal/insulator/metal (MIM) heterostructure. The detailed plasmonic dispersion characteristics have been investigated [3-5]. Many complicated designs of plasmon-based waveguide have also been proposed [6,7].

The plasmonic waveguides are often considered in the visible light and near-infrared, whereas the conventional waveguide modes reside in the microwave regime [8]. Despite the widely-studied plasmonic waveguides, previous works barely mentioned the transition of plasmonic modes between these two frequency ranges. To explore this subject, we focus on the MIM heterostructre in this paper. We demonstrate that given the metal dielectric at microwaves, the plasmonic modes over the MIM heterostructure can evolve into the conventional waveguide modes. In addition, the dispersion of a single SPP at a single metal/insulator boundary can be extracted from the transverse magnetic (TM) plasmonic modes. In doing so, the coupling effect of MIM plasmonic modes is clearly revealed. In fact, the symmetric and antisymmetric coupled SPP modes are associated with TEM (TM_0) and TM_1 guided modes, respectively.

It is worth to mention that earlier researches often employed negative dielectric or fitting to the relative permittivity function $\varepsilon_r(\omega) = 1 - \omega_p^2/\omega^2$, where ω_p is the angular plasma frequency, for the metal material in solving the plasmonic dispersion [4,5]. This approximation holds for near-infrared. Nevertheless, the permittivity is complex with extremely large imaginary part in the microwave regime. To truly reflect the reality, we adopt the Drude model with relaxation time (τ), which leads to large imaginary permittivity in microwaves.

2. Plasmonic Dispersion of the Metal/Insulator/Metal Structure

A metal/insulator interface is capable of guiding EM waves by exciting an SPP mode. The MIM heterostructure allows for two SPP modes accordingly. Due to the coupling of modes, the MIM is known to support coupled SPP modes, which are associated with symmetric/antisymmetric types [4]. In the microwave regime, the MIM structure, however, is related to the perfect-electric-conductor (PEC) parallel-plate waveguide, which supports a series of distinct waveguide modes [8]. In this section, we desire to illustrate how the plasmonic dispersion evolves into the conventional waveguide dispersion. A schematic of the MIM heterostructure is shown in Fig. 1(a). In the TM modes, the field components E_x, E_y, and H_z are presented. Directly solving the TM dispersion yields:

$$\frac{k_{xm}}{\varepsilon_m} = \frac{k_{xd}}{\varepsilon_d} j \cdot \begin{cases} -\tan(k_{xd}l) & \cdots \text{Symmetric} \\ +\cot(k_{xd}l)\ . & \cdots \text{Antisymmetric} \end{cases} \tag{1}$$

$$k_{xm}^2 + k_z^2 = \left(\frac{\omega}{c}\right)^2 \varepsilon_m$$
$$k_{xd}^2 + k_z^2 = \left(\frac{\omega}{c}\right)^2 \varepsilon_d \ . \tag{2}$$

Here k_{xm} (k_{xd}) is the complex wavenumber in metal (insulator) along the x-axis. Combining (1) and (2), the values of k_{xm}, k_{xd},, and k_z are determined with respect to ω. Consider the case that the half-distance l goes to infinity. It is easy to demonstrate

$$\tan(k_{xd}l) \to +j$$
$$\cot(k_{xd}l) \to -j \tag{3}$$

as $l \to \infty$. Note that (3) is valid for complex k_{xd}. Therefore, (1) becomes

$$\frac{k_{xm}}{\varepsilon_m} = \frac{k_{xd}}{\varepsilon_d} \ . \tag{4}$$

Substituting (4) into (2), we get

$$k_z = \frac{\omega}{c}\sqrt{\frac{\varepsilon_d \varepsilon_m}{\varepsilon_d + \varepsilon_m}} \ . \tag{5}$$

This is the well-known dispersion relation of the SPP mode. We thus conclude that (1) is the dispersion relation for the coupled SPP mode under the MIM heterostructure. Hence, (1) is also referred to as the plasmonic dispersion relation. The plasmonic dispersion has the limiting form of the single SPP dispersion when the distance between the two metal plates is assumed infinite. Here, we would like to point out that both "$-j\tan(k_{xd}l)$" and "$j\cot(k_{xd}l)$" are the coupling terms for the symmetric and antisymmetric cases, respectively.

Due to the periodicity of tangent/cotagent functions, (1) possesses a number of solutions. Next, we shall examine the plasmonic dispersion relation at the microwave frequencies, where the realistic metals are approximated as good or perfect conductors. We will see how (1) introduces TM- mode solutions and waveguide cutoffs. The Drude model takes the alternative form:

$$\varepsilon_m(\omega) = \varepsilon_0 \left(1 + \frac{j\sigma(\omega)}{\varepsilon_0 \omega}\right)$$
$$\sigma(\omega) = \frac{\sigma_0}{1 - j\omega\tau} \ , \tag{6}$$

where σ_0 is the DC conductivity, ε_0 is the vacuum permittivity, and τ is the relaxation time. Given the condition $\omega\tau \ll 1$, the conductivity $\sigma(\omega) \approx \sigma_0$ becomes frequency independent. A good/perfect conductor is approached if further making $\sigma_0 \gg \varepsilon_0\omega$. The Drude permittivity function then becomes $\varepsilon_m = \varepsilon_0 + j\sigma_0/\omega \approx j\sigma_0/\omega \to j\infty$. The perfect conductor is achieved using $\varepsilon_m \to j\infty$. Under this circumstance, the left-hand side of (1) reaches zero. The solutions making right-hand side zero are decomposed into three parts:

1) The TEM mode: $k_{xd} = 0$, so that

$$k_z = \sqrt{\varepsilon_d}\,\frac{\omega}{c} \ . \tag{7}$$

This is known as the TEM mode. It degenerates with the first-order solution of $\tan(k_{xd}l) = 0$, denoted by the TM_0 mode. Since $k_{xd} = 0$, this mode lacks cutoff. Note that the TEM mode is deduced from the TM dispersion, where the major electric field E_x is oriented orthogonal to the metal/insulator interface. The minor electric field E_z vanishes in this extreme case. Here, we would like to point out that the TEM mode can be treated as a special case of the symmetric coupled SPP mode. Figure 2(a), (b), and (c) illustrates the E_x field envelope of the TEM mode, the symmetric coupled SPP mode, and the single SPP mode, respectively. The solid line is the field envelope, and the dash-dotted line

is the boundary between metal and dielectric. The dash line in Fig. 2(b) denotes the before-coupling field amplitude.

2) The Higher-Order Symmetric TM Modes: $\tan(k_{xd}l) = 0$, so that

$$k_{xd}l = m'\pi \qquad (m' = 1,\ 2,\ 3, \cdots)$$
$$k_{xd} = \frac{m'\pi}{l}\ . \tag{8}$$

3) The Antisymmetric TM modes: $\cot(k_{xd}l) = 0$, so that

$$k_{xd}l = -\frac{\pi}{2} + m''\pi \qquad (m'' = 1,\ 2,\ 3, \cdots)$$
$$k_{xd} = -\frac{\pi}{2l} + \frac{m''\pi}{l}\ . \tag{9}$$

Combining (8) and (9) leads to

$$k_{xd} = \frac{m\pi}{2l} \qquad (m = 1,\ 2,\ 3, \cdots)\ . \tag{10}$$

Equation (10) is known to correspond to the TM-mode cutoffs for the PEC parallel-plate waveguide. Similar to the first-order symmetric solution, the TM_0 mode, the TM_1 mode (the first-order antisymmetric solution) results in the antisymmetric coupled SPP mode with finite dielectric thickness between metals. Figure 2(d), (e), and (f) plots the E_x field envelope of the TM_1 mode, the antisymmetric coupled SPP mode, and the single SPP mode, respectively. The SPPs at individual interfaces are coupled with opposite signs, leading to zero field at the coordinate origin. With PEC boundaries, the E_x field shows perfect sine function as in Fig. 2(d).

Shown in Fig. 1(b) is the dispersion curves calculated by (1), (3), and (5). The dash-dotted, dotted, and brown/red solid lines indicate the dispersion curves for the TEM mode, the single SPP mode, and the symmetric/antisymmetric coupled SPP mode, respectively. The dielectric with $\varepsilon_d = 1.96\varepsilon_0$ is sandwiched between two gold plates and $2l$ = 30 nm. The Drude parameters ω_p = 1365 THz and τ = 27.4 fs are used for the calculation. The single SPP and symmetric/antisymmetric coupled SPPs are all pinned at around $\omega_p/(\varepsilon_d+1)^{1/2}$, indicative of strong coupling to electrons, or so-called "plasma resonance." Moreover, the single SPP and symmetric coupled SPP modes show the asymptotic form: $k_z \sim \varepsilon_d^{1/2}\omega/c$ at very low frequencies, corresponding to the TEM mode.

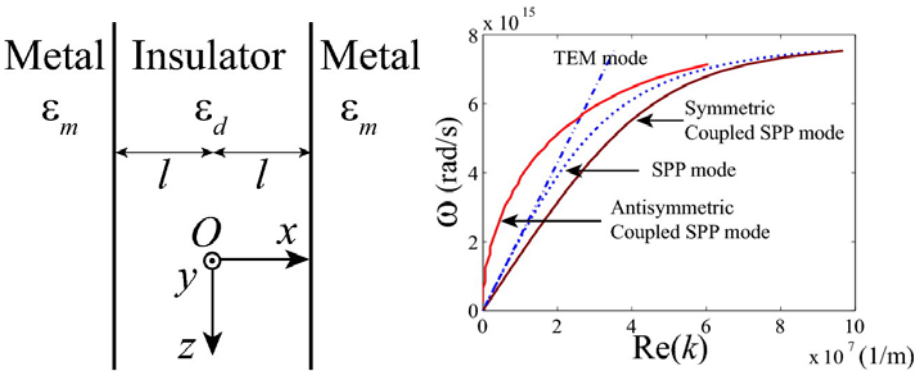

(a) (b)

Figure 1: (a) The geometrical plot of the metal/insulator/metal structure. (b) The dispersion curves of the TEM mode (dash-dotted line), the SPP mode (dotted line), and the symmetric/antisymmetric coupled SPP modes (brown/red solid lines).

3. TE Dispersion of the Metal/Insulator/Metal Structure

Following the standard derivation, one arrives at the dispersion relation of TE modes:

$$k_{xm} = k_{xd}\ j \cdot \{ \begin{array}{ll} -\tan(k_{xd}l) & \cdots \text{Symmetric} \\ +\cot(k_{xd}l) & \cdots \text{Antisymmetric} \end{array} \tag{11}$$

with H_x, H_y, and E_z taken into account. As $l \rightarrow \infty$, (11) results in $k_{xm} = k_{xd}$. Together with (2), we find that the solution does not exist. We thus conclude that the TE modes possess no plasmonic dispersion. Investigating the orientation of the electric field, the TM modes have their major component E_x orthogonal to the metal/insulator interface, while the TE modes have only E_z which is parallel to the interface. Recalling the single SPP dispersion, the dominant electric field component is required to be perpendicular to the boundary so that with which surface electrons are able to oscillate. The TE dispersion relation unfortunately shows no plasmonic solution since the surface electrons could by no means oscillate with parallel electric fields. With the perfect metal $\varepsilon_m \rightarrow j\infty$, it can be shown that $k_{xd} = m\pi/(2l)$, which corresponds to the cutoff conditions of TE modes for PEC parallel-plate waveguide at microwave frequencies.

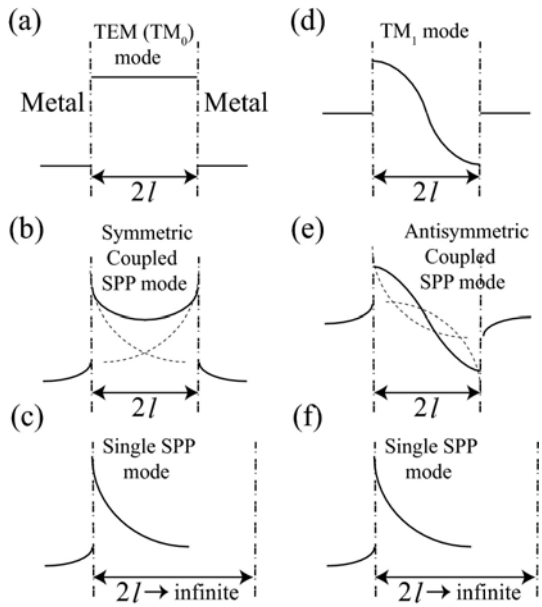

Figure 2: Illustration of the E_x field envelope of (a) the TEM mode, (b) the symmetric coupled SPP mode, (d) the TM_1 mode, (e) the antisymmetric coupled SPP mode, and (c), (f) the single SPP mode.

Acknowledgments

This work was supported in part by the National Science Council of the Republic of China under grant NSC96-2221-E-002-097, in part by the Excellent Research Projects of National Taiwan University under grant 95R0062-AE00-06, and in part by the Ministry of Education of the Republic of China under “The Aim of Top University Plan” grant.

References

[1] S. A. Maier, “Plasmonics: Metal Nanostructures for subwavelength Photonic Devices,” *IEEE J. Sel. Top. Quantum Electron*, vol. 12, pp. 1214–1220, 2006.

[2] S. A. Maier, M. L. Brongersma, P. G. Kik, S. Meltzer, A. A. G. Requicha, and H. A. Atwater, “Plasmonics—A route to nanoscale optical devices,” *Adv. Mater.*, vol. 13, p. 1501, 2001.

[3] K. R. Welford and J. R. Sambles, “Coupled surface plasmons in a symmetric system,” J. Mod. Opt., vol. 35, pp. 1467–1483, 1988.

[4] B. Prade, J. Y. Vinet, and A. Mysyrowicz, “Guided optical waves in planar heterostructures with negative dielectric constant,” *Phys. Rev. B*, vol. 44, pp 13556–13572, 1991.

[5] K. Y. Kim, Y. K. Cho, and H.-S. Tae, “Light transmission along dispersive plasmonic gap and its subwavelength guidance characteristics,” *Opt. Express*, vol. 14, pp. 320–330, 2006.

[6] G. Veronis and S. Fan, “Guided subwavelength plasmonic mode supported by a slot in a thin metal film,” *Opt. Lett.*, vol. 30, pp. 3359–3362, 2005.

[7] E. Moreno and F. J. Garcia-Vidal, “Channel palsmon-polaritons: modal shape, dispersion, and losses,”*Opt. Lett.*, vol. 31, pp. 3447–3449, 2006.

[8] D. M. Pozar, *Microwave Engineering*, New York, NY: John Wiley & Sons, 1998.